Inorganic Chemistry

Article

pubs.acs.org/IC

Stereochemistry of Complexes with Double and Triple Metal−Ligand Bonds: A Continuous Shape Measures Analysis

Santiago Alvarez,*[,†] Babil Menjón,[‡] Andrés Falceto,[†] David Casanova,[§,⊥,#] and Pere Alemany[∥]

[†]Departament de Química Inorgànica and [∥]Departament de Química Física, Institut de Química Teòrica i Computacional (IQTCUB), Universitat de Barcelona, Martí i Franquès, 1-11, 08028 Barcelona, Spain

[‡]Instituto de Síntesis Química y Catálisis Homogénea, CSIC−Universidad de Zaragoza, Pedro Cerbuna 12, E-50009 Zaragoza, Spain

[§]Kimika Fakultatea, Euskal Herriko Unibertsitatea (UPV/EHU), P.K: 1072, 20080 Donostia, Spain

[⊥]Donostia International Physics Center (DIPC), 20018 Donostia, Spain

[#]IKERBASQUE, Basque Foundation for Science, 48013 Bilbao, Spain

Supporting Information

ABSTRACT: To each coordination polyhedron we can associate a *normalized coordination polyhedron* that retains the angular orientation of the central atom−ligand bonds but has all the vertices at the same distance from the center. The use of shape measures of these normalized coordination polyhedra provides a simple and efficient way of discriminating angular and bond distance distortions from an ideal polyhedron. In this paper we explore the applications of such an approach to analyses of several stereochemical problems. Among others, we discuss how to discern the off-center displacement of the metal from metal−ligand bond shortening distortions in families of square planar biscarbene and octahedral dioxo complexes. The normalized polyhedron approach is also shown to be very useful to understand stereochemical trends with the help of shape maps, minimal distortion pathways, and ligand association/dissociation pathways, illustrated by the Berry and anti Berry distortions of triple-bonded [X≡ML$_4$] complexes, the square pyramidal geometries of Mo coordination polyhedra in oxido-reductases, the coordination geometries of actinyl complexes, and the tetrahedricity of heavy atom-substituted carbon centers.

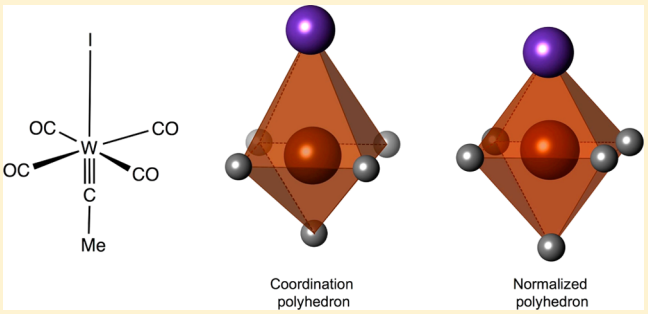

INTRODUCTION

The definition and application of shape and symmetry measures, especially to transition metal compounds, has been one of the goals of our research in the past few years. As part of that endeavor we have successfully proposed accurate stereochemical descriptions for the coordination spheres of thousands of transition metal complexes, by either attributing them one of the ideal polyhedral shapes commonly used or finding their position relative to a minimal distortion pathway between two ideal polyhedra.[1] In our early studies of the application of continuous shape measures to transition metal complexes we found that the usual differences in bond distances have a lesser effect on the shape measures of the coordination spheres, compared to angular distortions.[2] Bond length differences of up to 0.5 Å were explored and shape measures on the order of 2 units were observed, that were considered as being of little importance compared to the large shape measures that result from, e.g., a Bailar twist in a six-coordinate complex (16 units) or a flattening of a tetrahedral complex all the way to square planar (33 units).

Since the large knowledge accumulated comes mostly from complexes with single metal−ligand bonds, it is time now to take a closer look at molecules with large bond distance inequalities, including metal−ligand multiple bonds. What we are pursuing in this work is a sort of shape measure that allows us to easily recognize the angular distortions of a metal coordination polyhedron, disregarding those distortions that are due to bond length differences. To that end we define the *normalized coordination polyhedron* of the central metal in a given coordination compound as the polyhedron that results from normalizing all the metal−donor distances to the average of the bond distances while keeping the same spatial directions as in the real coordination polyhedron. We will briefly describe first the procedure used to generate normalized coordination polyhedra, then we will discuss a systematic approach to extract relevant chemical information from their shape measures, and finally we will apply the new methodology to the stereochemical analysis of several families of transition metal or actinide complexes with multiple metal−ligand bonds, as well as to a family of organic molecules.

Received: August 29, 2014
Published: November 3, 2014

   dx.doi.org/10.1021/ic5021077 | *Inorg. Chem.* 2014, 53, 12151−12163

PROCEDURE

To obtain a coordination polyhedron of a complex with normalized distances from the central atom to the vertices, the coordinates of the central atom and the N donor atoms are translated to place the central atom at the origin of coordinates. The coordinates of the donor atoms then define vectors pointing in the direction of the M-L bonds, whose modules are the bond distances. Those vectors are normalized to the average M-L bond distance (Chart 1):

$$\mathbf{r}_i^N = \frac{r_{av}}{r_i}\mathbf{r}_i;\ r_i = \sqrt{x_i^2 + y_i^2 + z_i^2} \qquad (1)$$

Chart 1

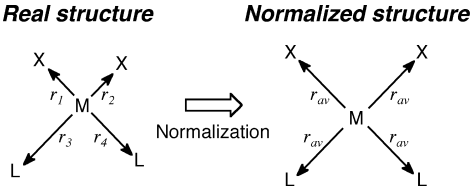

To make it clear when a shape measure refers to a normalized polyhedron, we will use from here on the symbol $S(^N\mathrm{P}, \mathrm{R})$ to denote the shape measure of a normalized coordination sphere P relative to a reference polyhedron R, where the second index will be omitted for simplicity when the reference polyhedron is clear from the context. It must be noted also that in this paper the word polyhedron may often refer to a coordination polygon, as in square planar complexes.

DISTORTIONS OF COORDINATION POLYHEDRA DUE TO MULTIPLE BONDING

In this section we show how the type of distortion of a coordination polyhedron induced by bond distance inequality can be analyzed with the help of three related shape measures relative to a given ideal polyhedron R: that of the coordination polyhedron itself, $S(\mathrm{ML}_n)$, the shape measure of the ligand shell, $S(\mathrm{L}_n)$, and the shape measure of the normalized coordination polyhedron, $S(^N\mathrm{ML}_n)$. For simplicity we take as an initial example for this preliminary discussion a two-dimensional system, a square planar $[\mathrm{MX_2L_2}]$ complex in which the M−X bonds are much shorter than the M−L ones. Once the procedure is established we will later apply it to a set of examples that includes tetrahedral and octahedral molecules as well.

When two *cis* bond distances are significantly shorter than the rest in *cis*-$[\mathrm{MX_2L_2}]$ complexes, the coordination sphere may present one of two alternative distortion modes, one that approaches the two X ligands to the metal atom (Figure 1a), without changing the bond angles around M, and another distortion produced by an off-center displacement of the metal toward an edge (Figure 1b) occupied by the shorter bonds. In the former case, the polygon defined by the donor atoms shell is distorted and therefore the shape measures of both the L_n envelope and the ML_n group should present relatively large values. Normalization of the coordination polygon, that consists simply of equalizing the bond distances without changing the directions of the metal−ligand bonds, recovers the perfect square with the metal atom at the center. This kind of distortion (Figure 1a) is therefore essentially characterized by a

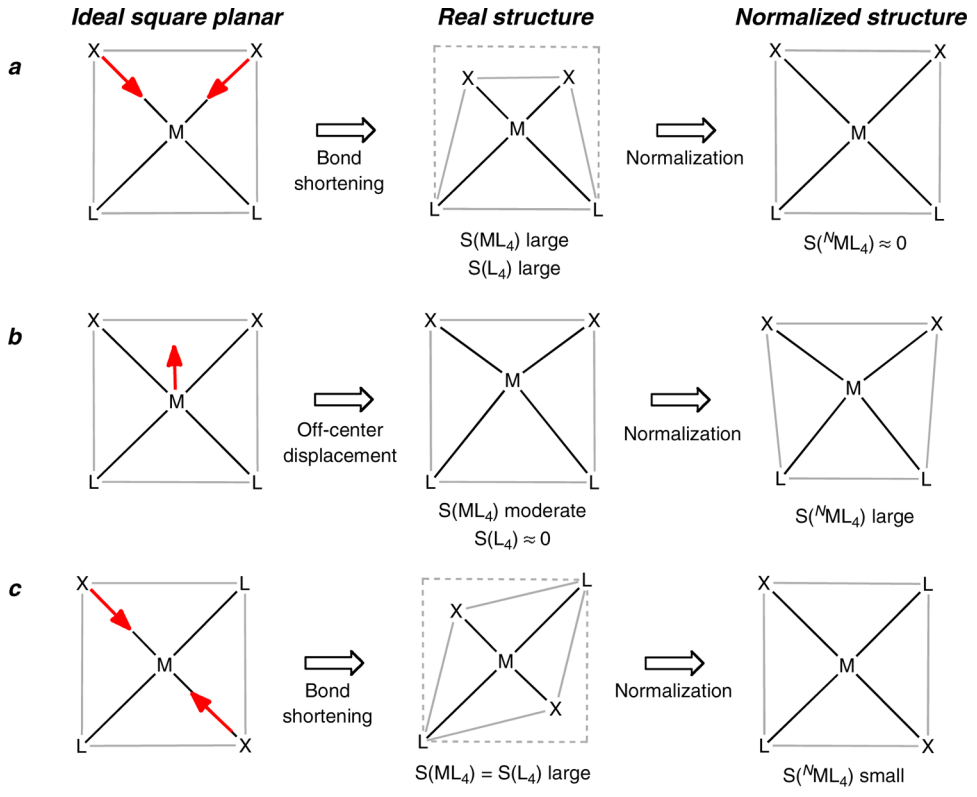

Figure 1. Schematic depiction of three types of distortion of a coordination sphere produced by strong bond distance inequalities, illustrated for the case of a square-planar $[\mathrm{MX_2L_2}]$ complex: a bond shortening (*a*), and an off-center displacement of the central atom (*b*) in the case of a *cis* arrangement of the two shortest bonds, and a bond shortening (*c*) for the *trans* arrangement. The expected magnitudes of the shape measures relative to the regular square are also indicated.

dx.doi.org/10.1021/ic5021077 | *Inorg. Chem.* 2014, 53, 12151−12163

Table 1. Shape Measures of the Experimental Coordination Polyhedra of Complexes of the Type $[MX_xL_y]$ with Very Short or Very Long M−X Bonds, $S(ML_n)$, and Their Changes upon Normalization $\Delta S(^NML_n)$, and upon Removal of the Central Atom, $\Delta S(L_n)$

x	y	compd.	polyhedron[a]	$S(ML_n)$	$\Delta S(^NML_n)$	$\Delta S(L_n)$	refcode	mode[c]
1	5	*trans*-$[WCMe(CO)_4I]$	OC-6	1.96	−1.95	−0.10	imcbcw[3]	**a**
1	5	*trans*-$[MoO(CN)_4(NCMe)]^{2-}$	OC-6	0.70	+0.66	−0.64	kodvoo[4]	**b**
2	2	$[VO_2Cl_2]^-$	T-4	2.27	−2.25	−0.14	phclov[5]	**a**
2	2	*trans*-$[OsO_2(P^iPr_3)_2]$	SP-4	2.56	−2.56	0.00	umazud[6]	**c**
2	2	*cis*-$[Pt(CEt(OEt))_2Cl_2]$	SP-4	0.56	−0.51	−0.13	yewcuz[7]	**a**
2	4	*cis*-$[MoO_2F_4]^{2-}$	OC-6	0.43	+0.44	−0.39	ihotop[8]	**b**
2	4	*trans*-$[OsO_2Cl_2py_2]$	OC-6	1.80	−1.61	0.00	juytus[9]	**c**
3	3	*fac*-$[ReO_3(Me_3tacn)]$[b]	OC-6	0.84	+0.76	−0.81	pidtol[10]	**b**

[a]Reference polyhedra: T-4 = tetrahedron, SP-4 = square, OC-6 = octahedron. [b]tacn = triazacyclononane. [c]For a depiction of the distortion modes **a**−**c**, see Figure 1.

dramatic decrease of the shape measure of the ML_n groups upon normalization (eq 2a).

The off-center displacement of the metal, on the other hand (Figure 1b), retains the square geometry of the coordination sphere but loses the centered square planar character of the MX_2L_2 group. Then, upon normalization, the coordination sphere becomes significantly distorted from the regular square, and the relationship between the three shape measures is expected to be the one expressed in eq 2b.

$$S(ML_n) > S(^NML_n) \quad (2a)$$

$$S(^NML_n) > S(ML_n) > S(L_n) \quad (2b)$$

$$S(ML_n) = S(L_n) > S(^NML_n) \quad (2c)$$

In those cases in which the two shortest (or the two longest) distances correspond to bonds in *trans* positions, one can expect only one type of distortion, i.e., an axial compression of the coordination polygon (Figure 1c). Since the metal remains at the center of the coordination sphere, the shape measures of the coordination polygon and that of the ligand shell must be identical and nonzero, whereas normalization restores the regular square and results in the shape measures distribution indicated in eq 2c.

Similar considerations apply to $[MXL_3]$ complexes, in which one can foresee either an off-center shift toward the vertex X, or an M−X bond shortening that keeps the metal atom at the center of the square. For octahedral *fac*-$[MX_3L_3]$ molecules one can also think of a metal shift toward a face and of the alternative approach of the X ligands to the center of the octahedron.

In summary, we can establish the simple rule that a decrease in the shape measure of a coordination polyhedron upon normalization is indicative of a bond shortening (or lengthening) distortion that preserves the bond angles of the ideal polyhedron, whereas an increase is diagnostic for an off-center shift of the central atom that makes the bond angles around it different than in the reference polyhedron. In the latter case, one can add that the shape measure of the donor atoms shell must be smaller than that of the whole coordination sphere. To illustrate how this simple rule works, we show in Table 1 and Figure 2 a few examples and propose to the reader to deduce which of the three types of distortion is present in each particular example. To facilitate the task, we present in Table 1 the changes in the polyhedral shape measured upon polyhedral normalization, $\Delta S(^NML_n)$, and upon removal of the central metal atom, $\Delta S(L_n)$.

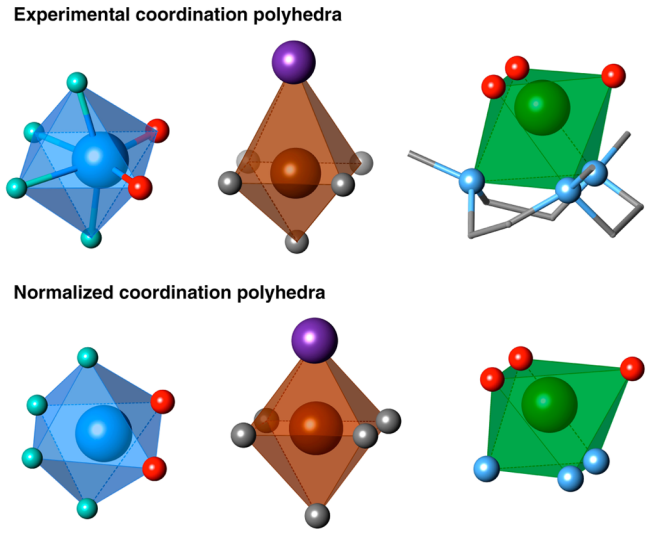

Figure 2. Experimental and normalized coordination polyhedra of $[MoO_2F_4]^{2-}$ (ihotop, left),[8] *trans*-$[WCMe(CO)_4I]$ (imcbcw, center),[3] and *fac*-$[ReO_3(Me_3tacn)]$ (pidtol, right).[10]

Besides the simplest cases discussed so far, there are two additional possibilities to be considered. First, we can find a combination of shorter bonds in one direction and elongated bonds in another direction, as in $[MoO_2Br_2(dmso)_2]$ (Figure 3).[11] Since the distortion associated with the two short Mo═O bonds in *cis* makes the shape measure for the normalized polyhedron higher than for the original one (eq 2b), while the two long Mo−Br distances in *trans* favor a decrease of the shape measure upon normalization, it is not straightforward to predict what will be the change of the octahedral shape measures for that compound upon normalization. We find,

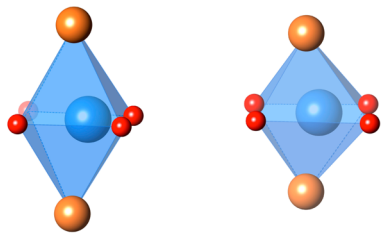

Figure 3. Experimental (left) and normalized (right) coordination polyhedron of *trans*-$[MoO_2Br_2(dmso)_2]$ with two short Mo═O, two intermediate Mo−O, and two long Mo−Br bonds.[11]

dx.doi.org/10.1021/ic5021077 | *Inorg. Chem.* 2014, 53, 12151−12163

however, that it becomes smaller, indicating the predominance of the Mo═O bond shortening distortion. Second, a strong bond distance inequality may be combined with an angular distortion, such as a Bailar twist, an issue to which we will come back later in the analysis of specific families of complexes.

One could envisage carrying out continuous symmetry measures of normalized polyhedra, even if the analysis of minimal distortion pathways with symmetry measures has been less developed than with shape measures. To give just a glimpse of an alternative approach for the systems studied in this section, we have calculated the inversion symmetry measures of those compounds in Table 1 that are potentially centrosymmetric (see Supporting Information Table S1), and we have found that the ones with bond shortening distortion (**a** in Figure 1 and in Table 1) present a substantial decrease in their inversion measure upon normalization, while those with an off-center shift of the metal atom increase their inversion measure, and *trans*-$[OsO_2(P^iPr_3)_2]$ presents inversion symmetry in both its experimental and normalized coordination polyhedra. From here on we will limit our analysis to shape measures for simplicity.

A. Square Planar *cis*-$[MX_2L_2]$ Complexes. We start by analyzing a family of square planar complexes, since distortions in the plane are easier to visualize than in three dimensions. Consider the *cis*-$[MX_2L_2]$ complexes in which the ligands X form double bonds to the metal and therefore present significantly shorter M−X than M−L bond distances. We choose the group 10 carbene complexes of the type shown in Figure 4, restricted to those cases in which the M═C and M−L bonds are acyclic to disregard angular distortions imposed by bidentate ligands.[7,12,13] The three relevant shape measures for each of the five crystallographically independent molecules found are represented in a square-tetrahedron shape map (Figure 4).

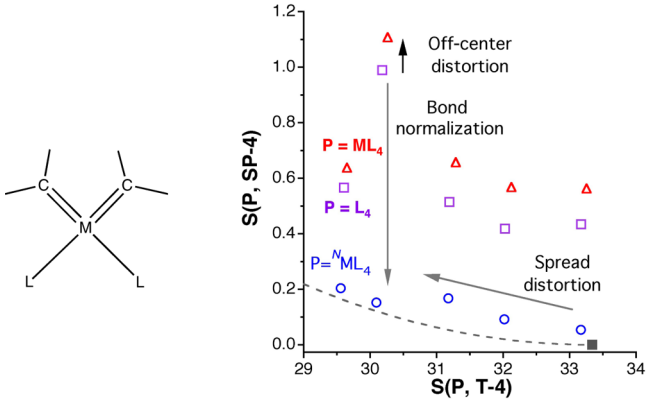

Figure 4. Shape measures of square planar *cis*-biscarbene complexes relative to the tetrahedron (T-4) and the regular square (SP-4), for the experimental coordination sphere (triangles), for only the donor atoms in the experimental structure (open squares), and for the normalized coordination sphere (circles). The position of the perfect square in this shape map is indicated by a solid square at the bottom.

The rightmost points in Figure 4, which correspond to $[Pt(C\{COMe\}Et)_2Cl_2]$,[7] indicate that its normalized coordination sphere is close to a regular square and therefore that the distortion of the coordination sphere in this compound is mostly of the bond shortening type (Figure 1a and eq 2a). If we look at the other members of this family now, the main difference is that their normalized coordination spheres are farther from the square (i.e., from $S(^NML_4, SP\text{-}4) = 0$), but close to the minimal distortion pathway between the square and the tetrahedron (dashed line in Figure 4). In other words, these complexes combine a bond distance distortion with some degree of tetrahedralization, of up to 7% in an N-heterocyclic carbene complex[13] and a bit larger (10%) for a nickel(II) complex with a bidentate bis-N-heterocyclic carbene ligand[14] (not shown in Figure 4). It must also be stressed that, were we looking at the shape measures of the experimental coordination spheres, we might have concluded simply that the palladium complex represented by the highest point in Figure 4 is significantly more distorted than the rest of the structures analyzed. However, the analysis of the normalized polyhedra clearly reveals that the deviation from the square is essentially due to the presence of longer Pd−Br distances, but the angular distribution of the donor atoms is similar to the other members of the family and places it at the early stages of the spread distortion that converts the square into a tetrahedron. These results show the usefulness of the normalization strategy that allows us to uncover the alignment of these structures along the spread pathway amidst the prevalent bond distance distortion in the experimental coordination spheres.

B. Octahedral *cis*-$[MO_2L_4]$ Complexes. An obvious extension of this analysis to three-dimensional molecules takes us to the family of *cis*-$[MO_2L_4]$ complexes with two double-bonded oxo ligands. Since the metal atoms in these complexes are in the equatorial plane (the one that contains the two M═O bonds), we analyze first the equatorial MO_2L_2 group to check whether the distortion from the ideal octahedron within that plane corresponds to an off-center shift of the metal atom toward the O_2 edge that would leave a regular O_2L_2 square (Figure 1b), or to a bond shortening distortion that approaches that edge to the metal, thus deforming the O_2L_2 square to a trapezoid (Figure 1a). To illustrate this point we have chosen three examples of *cis*-dioxo complexes: $[MoO_2F_4]^{2-}$ (Figure 2),[8] $[MoO_2Cl_2(dmso)_2]$,[15] and $[MoO_2Br_2(dmso)_2]$[11] (Figure 3), and the results are represented in Figure 5. All these examples show the same behavior in the equatorial plane: $0 \approx S(L_4, SP\text{-}4) < S(ML_4, SP\text{-}4)$, indicating an off-center shift of the metal atom within a

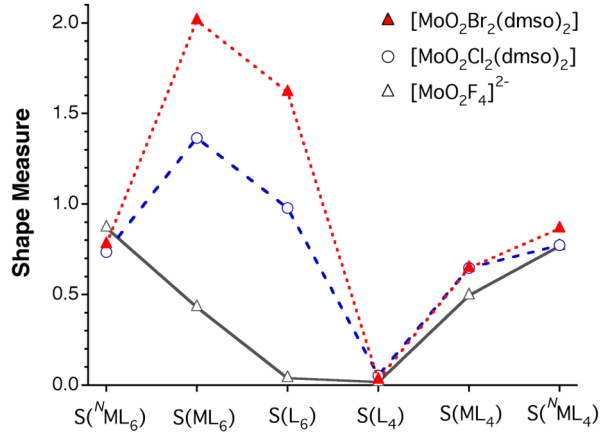

Figure 5. Octahedral shape measures of the *cis*-dioxo complexes $[MoO_2F_4]^{2-}$,[8] $[MoO_2Cl_2(dmso)_2]$,[15] and $[MoO_2Br_2(dmso)_2]$[11] for their coordination polyhedra, $S(ML_6)$, normalized coordination polyhedra, $S(^NML_6)$, polyhedral ligand cage, $S(L_6)$, and the corresponding square planar shape measures for the equatorial MO_2L_2 group, $S(ML_4)$, $S(^NML_4)$, and $S(L_4)$.

dx.doi.org/10.1021/ic5021077 | *Inorg. Chem.* 2014, 53, 12151−12163

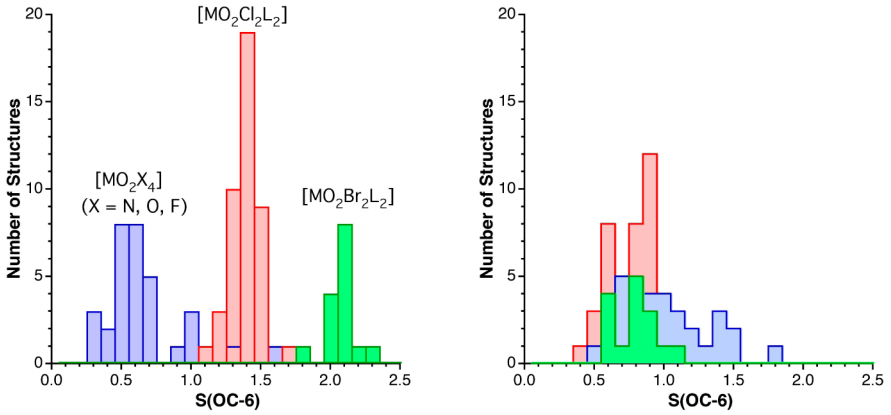

Figure 6. Distribution of the octahedral shape measures of the ML_6 group (left) and of the normalized ML_6 polyhedra (right) for the families of *cis* complexes $[MO_2X_4]$, $[MO_2Cl_2L_2]$ and $[MO_2Br_2L_2]$ (M = Mo, W; X = N-, O-, or F-donor ligands).

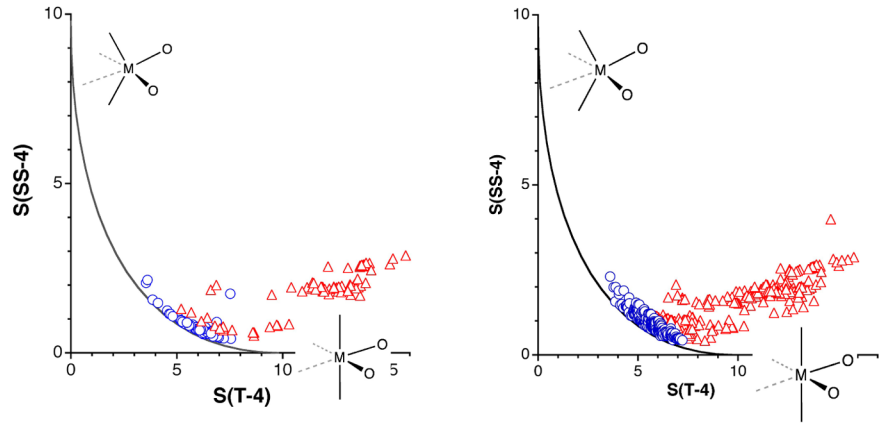

Figure 7. Tetrahedral to *cis*-divacant octahedral shape maps for the $MO_2^{ax}L_2$ group in *cis*-$[MO_2L_4]$ complexes (M = Mo, W) with monodentate ligands only (left, 76 data sets) and including chelating ligands (right, 234 data sets). Triangles correspond to the experimental coordination polyhedra, circles to the normalized polyhedra that fall within 10% of the minimal distortion path (91% of the sample). The insets show the ideal geometries at S(SS-4) = 0 and S(T-4) = 0, respectively.

nearly regular square cage formed by the equatorial ligands (see Figure 1b and eq 2b).

Contrary to the similar behavior of the equatorial MO_2L_2 groups of these three complexes, the octahedral shape measures of their full $MoO_2L_2X_2$ coordination polyhedra present two different trends (Figure 5). First, their S(ML_6) shape measures indicate varying degrees of distortion, with the fluoro complex being close to a perfect octahedron while the chloro and bromo examples show higher deviations from regularity. Those shape measures decrease upon removal of the central metal atom, indicating the off-center position of that atom within the coordination polyhedron. Finally, if we look at the normalized coordination polyhedra, they all have similar octahedral measures, that reflect the similar spatial orientation of their metal–ligand bonds. Three conclusions follow: (i) these three complexes present similar off-center shifts of the metal atoms within the equatorial plane; (ii) they show different degrees of bond distance inequalities, associated with the size of the axial ligand X, in the order F < Cl < Br, as expected from the covalent radii of those elements, relative to that of the other four oxygen donor atoms; and (iii) the three complexes have similar angular distributions of the bond angles around the metal atom that deviate from those expected for a regular octahedron.

To analyze the angular distortion found above for a small sample of *cis*-$[MoO_2X_2L_2]$ complexes, we now zoom out to cover all that family of complexes. We observe that the octahedral measures of their coordination spheres (Figure 6) can be roughly grouped in three families: (a) complexes with X donor atoms of the first long period (N, O or F) give small shape measures, (b) complexes with X = Cl give intermediate values, and (c) complexes with X = Br give large values. The normalized coordination spheres of the three families, however, reveal similar degrees of distortion from the regular octahedron, clearly indicating that they differ from each other mostly in their bond distance distributions, as found in the three examples just analyzed. A look at the experimental bond angles around the metal atoms confirms that their distributions are indeed quite similar for the three families of complexes. The next issue we should address is thus which is the angular distortion left over after polyhedra normalization has removed bond stretch distortions.

In these compounds, the bending of the two axial ligands away from the two M=O double bonds and the relatively long distances of the two equatorial ligands in *trans* suggest that these structures could be defined as snapshots along the ligand dissociation path that goes from the octahedron to the tetrahedron.[16] Such a pathway can be analyzed by mapping the shape measures of the $MO_2^{ax}L_2$ group with respect to the

dx.doi.org/10.1021/ic5021077 | *Inorg. Chem.* 2014, 53, 12151–12163

cis-divacant octahedron (also called a seesaw) and the tetrahedron, presented in Figure 7 for structures of Mo and W compounds retrieved from the Cambridge Structural Database (CSD)[17] and for three solid state structures from the Inorganic Crystal Structure Database (ICSD).[18] In that plot it can be seen that, while most of the coordination polyhedra cannot be reasonably described as falling along the octahedral-to-tetrahedral dissociation path, 91% of those fragments of the corresponding normalized polyhedra deviate, at most, 10% from it. A similar analysis for all transition metals (5239 structural data sets, Supporting Information Figure S1) showed also that only 48% of the ML_4 fragments are within 10% of the minimal distortion path between the tetrahedron and the divacant octahedron for the experimental structures, but it increases to 91% when the normalized polyhedra are considered.

C. Octahedral *trans*-[MO_2L_4] Complexes. One can easily figure out that the presence of two short M═O bonds in *trans* positions of an octahedron should result in a compressed tetragonal bipyramid. That this is the main distortion of the octahedral coordination sphere in the family of *trans*-[MO_2L_4] complexes can be seen by comparing the distribution of octahedral shape measures for both the experimental and normalized coordination polyhedra (Figure 8). Consistently, the octahedral shape measures of the ML_6 group and of the L_6 ligand envelope are quite similar in those cases.

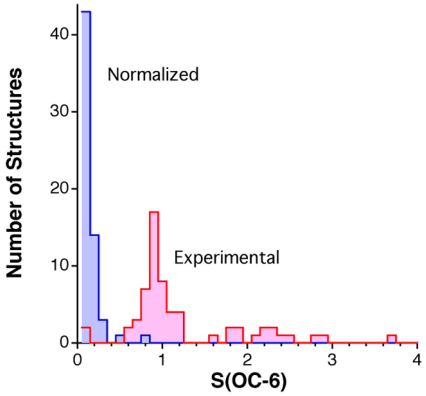

Figure 8. Distribution of octahedral shape measures of the *trans*-[MO_2L_4] complexes with monodentate ligands. The rightmost (pink) bins correspond to the experimental and the leftmost (blue) ones to the normalized coordination spheres.

D. Octahedral [X═ML_5] and *trans*-[X≡MYL_4] Complexes. In this section we consider six-coordinate complexes with a double or triple-bonded atom (X = C, N, O, P, S, or Se). Now that we have shown that bond distance normalization results in shape measures that better describe the spatial orientation of the metal−ligand bonds, we continue our discussion in this section by making use of only the normalized polyhedra for simplicity. If we look first at compounds with only monodentate ligands, we see how they cluster at the early stages of a Bailar distortion[2] of the octahedron (Figure 9, left). When bi- and multidentate ligands are included in the search, three main changes are found (Figure 9, right): (i) A larger portion of the Bailar path is covered. (ii) Two structures appear as practically perfect trigonal prismatic: an oxo Nb phthalocyanine derivative,[19] and a Mo dithiolene carbene complex.[20] (iii) There is much wider dispersion of the points, with many structures significantly deviating from the Bailar pathway.

To analyze the distortions present in the non-Bailar compounds of this family we have taken the subset of structures that deviate 20.0% or more from the Bailar path (74% of the full data set). If we disregard the ligand *trans* to the M−X multiple bond, we find more than half of those structures along a pyramidalization path that takes a vacant octahedral $XM^{eq}L_4$ fragment to a square pyramidal geometry (Figure 10, left). That path represents a distortion of the octahedron to a square pyramid with a partially dissociated ligand *trans* to the multiple-bonded X ligand.

Another set of compounds that present non-Bailar structures (Supporting Information Figure S2) are found to be aligned along the path that goes from the octahedron to the pentagonal pyramid (Figure 10, right). In all complexes with large distortions toward the pentagonal pyramid the donor atom *trans* to X belongs to a chelating ligand with a small bite angle that pulls it toward an equatorial position. Among the compounds that appear very close to the pentagonal pyramid, represented by points with $S(^{N}OC\text{-}6)$ between 19.0 and 30.0, we see one that falls right on the path. It has the formula [N≡Mo(terpy)$(N_3)_2$],[21] and showcases an incipient Mo−N bond (2.456 Å) with an azido group from a neighboring molecule, at a significantly long distance compared to the intramolecular Mo−N_3 bond lengths of 2.075 and 2.120 Å. This result suggests that the distortion toward a pentagonal pyramid opens up a seventh coordination site and may facilitate ligand association reactions. The compound closest to a perfect pentagonal pyramid is the $[O{\equiv}Nb(C_6F_5)_5]^{2-}$ anion.[22] Finally, a group of points close to the pentagonal pyramid but somewhat separated from the minimal distortion path correspond to ligands that form three-member chelate rings, mostly peroxo, disulfido, and diselenido ligands. It must be reminded that for small distortions of the octahedron (i.e., for the structures at the octahedral end of the minimal distortion pathways of Figures 9 and 10) it is not simple to decide from simple inspection of the shape maps which is the distortion presented by a given structure. Therefore, many nearly octahedral structures may appear in more than one plot. However, the structures at the distant end of the path can be unequivocally assigned to the particular path from which they deviate little.

E. Five-Coordinate [X≡ML_4] and [X═ML_4] Complexes. The five-coordinate complexes with one double or triple metal−ligand bond behave in similar ways, with the structures concentrated along the Berry pseudorotation pathway (Figure 11), a trend that is only apparent after normalization of the coordination polyhedra. Among the complexes with a triple-bonded atom, those that are closer to the trigonal bipyramid may have that atom in an axial or an equatorial position of the trigonal bipyramid, whereas for most part of the interconversion path the triple bond occupies an equatorial position of the trigonal bipyramid that ends up at an apical position of the square pyramid. In some of the trigonal bipyramids with axial triple bond there is also an off-center displacement of the metal atom from the equatorial plane, away from the multiple-bonded ligand tracing an umbrella distortion path.[27]

F. Dioxo Five-Coordinate Complexes *cis*-[MO_2L_3]. The $[MoO_2(C_6F_5)_3]^-$ anion[28] offers a good example of how the combined use of normalized coordination polyhedra and association/dissociation pathways can provide a clear stereo-

dx.doi.org/10.1021/ic5021077 | *Inorg. Chem.* 2014, 53, 12151−12163

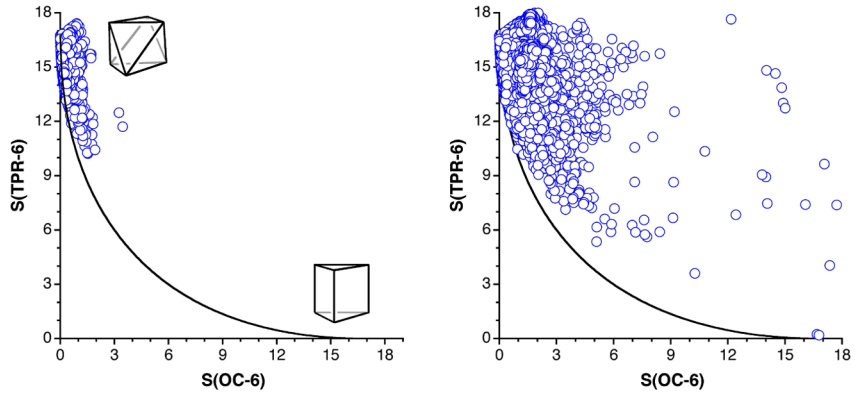

Figure 9. Left: Shape measures for the normalized coordination polyhedra of [X≡ML_5] and [X═ML_5] complexes with monodentate ligands only, plotted on a shape map for the interconversion between the octahedron and the trigonal prism. Right: Analogous map for all complexes, including bi- and multidentate ligands (33 321 data set).

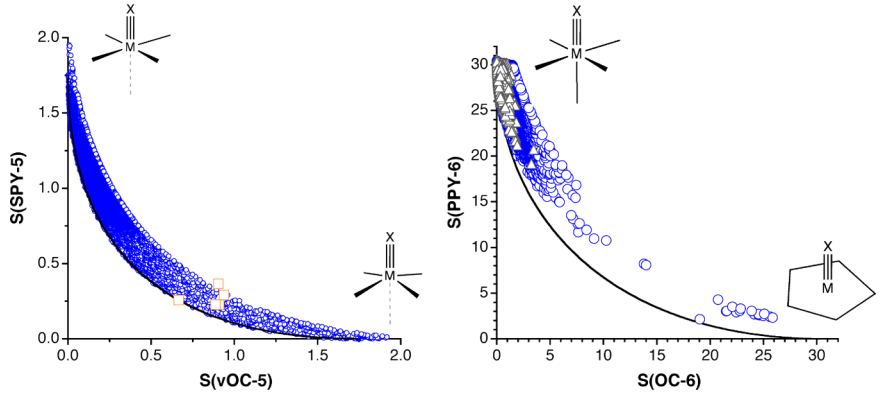

Figure 10. Left: Shape measures for the normalized coordination polyhedra of the XML_4 fragment of [X≡ML_5] and [X═ML_5] complexes that deviate at most 15% from vacant octahedron to square pyramid pathway (14 463 data set), omitting the ligand *trans* to X, and including some solid state compounds (squares: $MoOF_4$,[23] $NaKMoO_2F_4$,[24] $MoOCl_4$,[25] and $RbVOF_3$[26]). Right: Shape map for the [X≡ML_5] and [X═ML_5] complexes (circles; compounds with monodentate ligands only are represented by triangles) that deviate less than 20.0% from the minimal distortion path between the octahedron and the pentagonal pyramid.

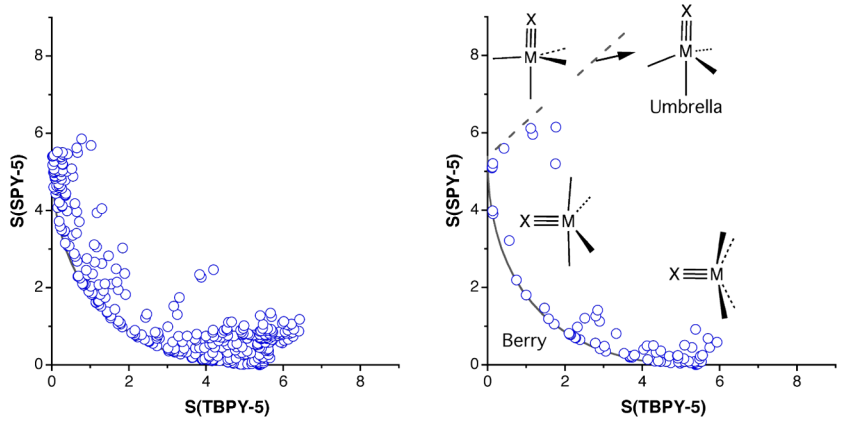

Figure 11. Shape map for the normalized coordination polyhedra of [X═ML_4] (left) and [X≡ML_4] (right) complexes (X = C, N, O, Si, P, or S-donor ligand) compared with the Berry (continuous line) and umbrella (dashed line) distortions of the trigonal bipyramid.

chemical description of apparently odd structures. A shape analysis of its experimental coordination polyhedron gives trigonal bipyramidal and square pyramidal shape measures of 2.60 and 4.23, respectively, too large to identify it with either of those ideal polyhedra. The corresponding normalized coordination polyhedron gives smaller shape measures (2.00 for the trigonal bipyramid and 3.59 for the square pyramid), but still too large for an unambiguous stereochemical assignment. A look at the deviation functions[29] of the normalized polyhedron from the minimal distortion interconversion pathway between the trigonal biyramid and the square pyramid[27] (44%) indicates that its deviation from the ideal polyhedra cannot be attributed to a Berry distortion. We observed that, contrary to what one would expect for a Berry distortion of the trigonal bipyramid, the ^{ax}L-M-^{eq}L bond angles (76°) are significantly smaller than 90° and also the O═M═O bond angles (113.6°) are smaller

dx.doi.org/10.1021/ic5021077 | *Inorg. Chem.* 2014, 53, 12151−12163

than what should be expected for a trigonal bipyramid. We are thus facing an anti-Berry distortion (Chart 2) that can be

Chart 2

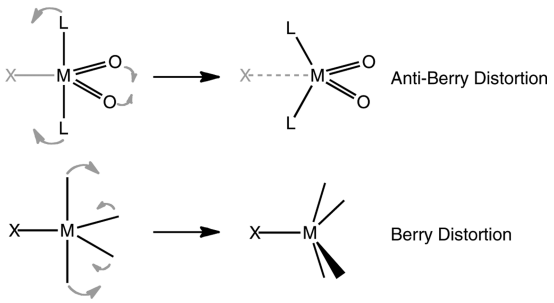

thought of as being along the pathway for the dissociation of an equatorial X ligand in a trigonal bipyramid to render a tetrahedral complex, which could be alternatively described as an edge-capped tetrahedron.

We therefore decided to carry out a shape analysis for the MoO_2C_2 fragment common to the five- and four-coordinate extremes of the dissociation pathway, comparing it with the equatorially vacant trigonal bipramid (eqvTBPY-4) and the tetrahedron (T-4) in a shape map. While the position of the real coordination polyhedron in that map (Supporting Information Figure S3) is far from the minimal distortion path, the normalized polyhedron falls practically along the dissociation path that goes from the trigonal bipyramid to the tetrahedron, 41% along the way.

Having found the structure of the $[MoO_2(C_6F_5)_3]^-$ anion to be along the anti-Berry pathway, we will apply now the same analysis to all known five coordinate complexes with two M═O double bonds. We start by looking at only those complexes with monodentate L ligands to avoid the results being affected by angular constraints imposed by bi- or multidentate ligands. The results (Figure 12) clearly show that the normalized coordination polyhedra of a variety of complexes fall along the anti-Berry pathway, but a number of structures do not correspond to that type of distortion, presenting tetrahedral shape measures of the $MO_2(^{ax}L)_2$ fragment in excess of 15. The line at high S(T-4) values corresponds instead to the Berry pathway. A closer look at the oxidation states of the metals reveals that all the anti-Berry structures pertain to the d^0 electron configuration (V^V, Mo^{VI}, W^{VI}, Re^{VII}, and Tc^{VII}) whereas the Berry structures are all of d^2 complexes (Tc^V, Re^V, Ru^{VI}, Os^{VI}). The only case that presents a regular trigonal bipyramidal geometry, at S(T-4) ≈ 12, is $[VO_2F(t\text{BuPyrazoly})_2]$.[30] A point that stands out of the Berry-anti Berry pathway, at S(T-4) ≈ 12, corresponds to the normalized coordination polyhedron of $[ReO_2(\text{neopentyl})_3]$,[31] an approximately trigonal bipyramidal structure that is distorted due to agostic interactions between the three neopentyl groups and the Re atom at Re···H ≈ 2.6 Å.

Density functional theory (DFT) calculations on several Mo^{VI} and Ru^{VI} dioxo complexes reproduce the experimental trend (Figure 12): the d^0-Mo^{VI} compounds present anti Berry geometries, while the d^2-Ru^{VI} complexes exhibit Berry distortions (Supporting Information). Interestingly, the optimized structure of $[RuO_2Me_3]^-$ presents agostic interactions for the two axial methyl groups, taking it away from both the Berry and anti-Berry pathways. Tatsumi and Hoffmann explained the tendency to bending away from the two oxo ligands in molybdenyl complexes in terms of "maximum utilization of vacant d orbitals in π bonding with oxygen lone pairs".[32] A closer look at the vacant d_{yz} orbital in $[MoO_2Ph_3]^-$ clearly shows its enhanced Mo−O π antibonding character thanks to the rehybridization induced by the non linear L_{ax}-Mo-L_{ax} group (Figure 13, left), but also indicates that it becomes involved in σ bonding with the axial ligands. In the analogous ruthenium (VI) complex, occupation of that d orbital requires it to have nonbonding character, which is achieved by bending the L_{ax}-Ru-L_{ax} unit toward the oxygen atoms and by opening up the O═M═O bond angle (Figure 13, right).

G. Molybdenum Oxido-Reductases. The important class of molybdenum oxidoreductases includes sulfite oxidases, xanthine oxidases, and dimethyl sulfoxide reductases.[33] All of them contain a molybdenum cofactor in which a molybdenum ion is coordinated by one or two pyranopterin-dithiolene ligands, and whose stereochemical and electronic properties are crucial for their enzymatic activity. Given the rich structural chemistry of this class of compounds,[34] we have examined over 100 pentacoordinated molybdenum sites in oxidoreductases which present a variety of distributions of single and double bonds. The structural motifs found (Chart 3) comprise **1a** with

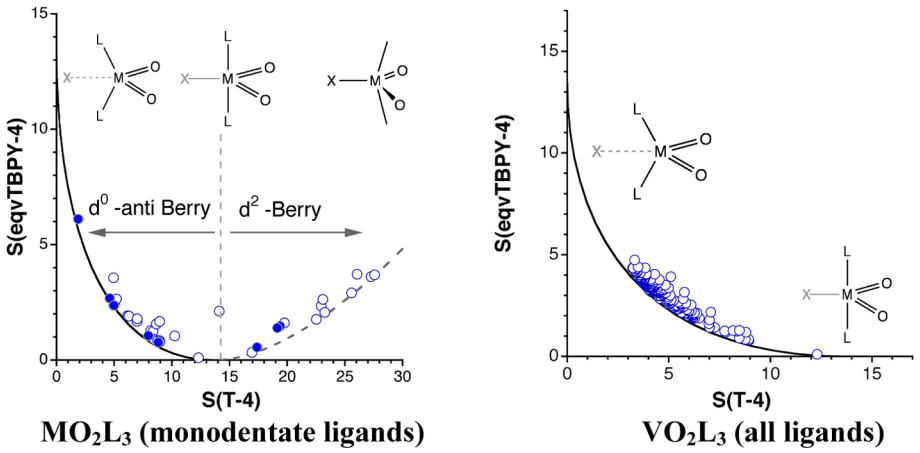

Figure 12. Left: Position in a shape map of the normalized coordination polyhedra of $[MO_2L_3]$ complexes with monodentate ligands found in the CSD (open circles) and of several computationally optimized structures (filled circles). Right: Similar shape map for all $[VO_2L_3]$ complexes, regardless of the denticity of their ligands.

dx.doi.org/10.1021/ic5021077 | Inorg. Chem. 2014, 53, 12151−12163

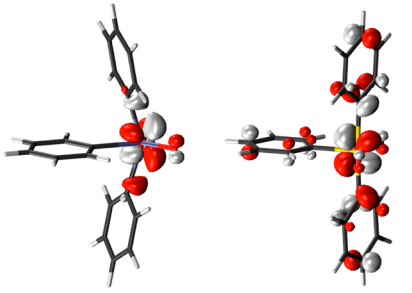

Figure 13. Lowest energy d-block molecular orbital $[MoO_2Ph_3]^-$ and $[RuO_2Ph_3]^-$ presenting different degrees of axial σ antibonding and equatorial π antibonding character. The geometrical parameters given correspond to the optimized structures.

Chart 3

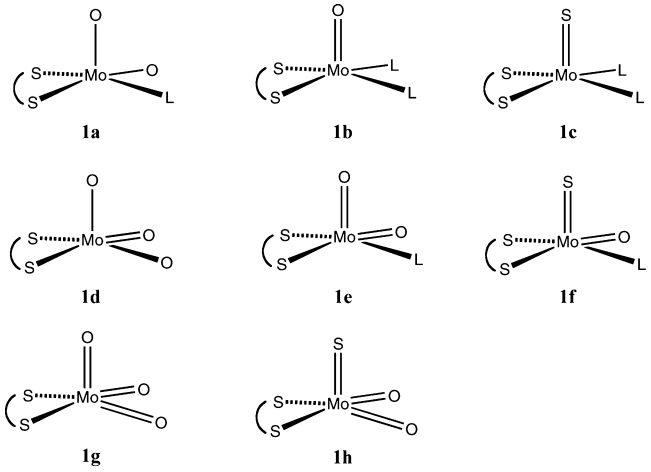

five single bonds,[35] **1b** with one apical double bond to an oxygen[36−38] or the sulfido analogues **1c**,[39,40] **1d** with an oxo ligand in a basal position,[41] **1e**[37,42] and **1f**[40] with two double bonds to apical and basal ligands, and even **1g**[43] and **1h** with three double bonds (Chart 3).[44]

The use of normalized polyhedra allows us to analyze the stereochemistry of those molybdenum sites on the same footing, regardless of the number and arrangement of metal−ligand double bonds. The square pyramidal measures of those structures are biased by the bond distance inequalities, but polyhedral normalization renders a clear overall stereochemical picture (Figure 14, left): the shapes of those sites are concentrated near the square pyramid. The representation of a shape map (Figure 14, right), however, tells us that a number of structures significantly deviate from the square pyramid, a distortion that cannot be associated with Berry pseudorotations, and only in two sites[38,45] has the Mo environment a stereochemistry roughly intermediate between the square pyramid and the trigonal bipyramid. The strong non-Berry deviations from the square pyramid are due to marked asymmetry in bond angle distribution, or to weak coordination of a nearby atom. As an example, the uppermost point in Figure 14 (right) corresponds to a Mo site that is semichelated by a carboxylato group.[46] The stereochemical behavior of these molybdenum sites is at odds with that shown by molecular complexes of the type $[X{=}Mo(dithiolene)_2]$ that appear nicely aligned along the Berry pathway (see Supporting Information Figure S4).

H. Four-Coordinate $[X{\equiv}ML_3]$ Complexes (X = C, N, P). In this family of four coordinate $[X{\equiv}ML_3]$ complexes (M = V, Nb, Cr, Mo, W) the normalized coordination polyhedra are nicely aligned along the interconversion pathway between the tetrahedron and the axially vacant trigonal bipyramid (Figure 15). In other words, the X−M−L bond angles vary between the tetrahedral angle and 100°. The highest point in the map, with S(vTBPY-4) ≈ 4, corresponds to the structure of an imido Nb^V compound[47] with one wide angle of 117°.

I. Uranyl and Actinyl Complexes. The uranyl group, UO_2^{2+} is ubiquitous in the chemistry of uranium (VI), but U=O double bonds also exist in uranium compounds with lower oxidation states. The uranium atoms adopt a variety of coordination numbers and coordination geometries,[48] including ill-defined coordination numbers and geometries along polyhedral interconversion paths.[49] Those characteristics make the uranium complexes in general an ideal case for the use of normalized polyhedra, a study that can also be applied to other actinides.

If we start with six-coordinate complexes of type $[UO_2L_4]$, where L is a monodentate ligand, their experimental

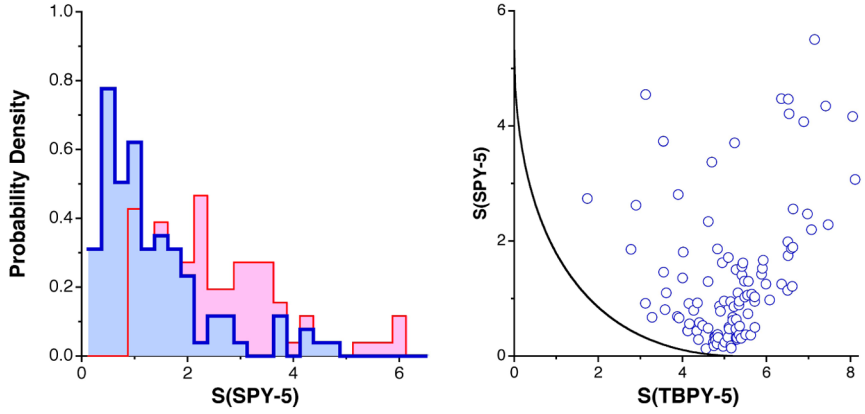

Figure 14. Left: Distribution of the square pyramidal shapes of the pentacoordinated molybdenum sites in oxidoreductases, considering their experimental (pink bins) and normalized (blue bins) coordination polyhedra. Right: Shape map for their normalized polyhedra relative to the trigonal bipyramid (TBPY-5) and the square pyramid (SPY-5), with the Berry pseudorotation pathway shown as reference (continuous line).

dx.doi.org/10.1021/ic5021077 | Inorg. Chem. 2014, 53, 12151−12163

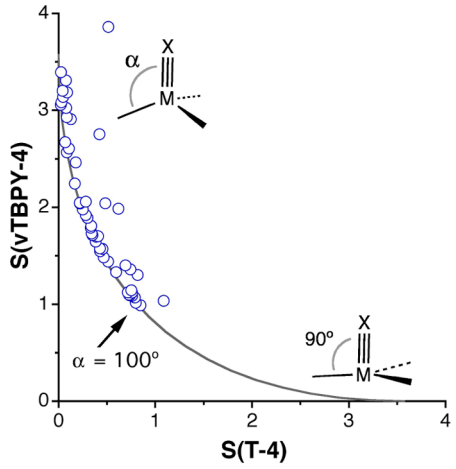

Figure 15. Shape measures of the normalized coordination polyhedra of triply bonded $[X{\equiv}ML_3]$ complexes relative to the tetrahedron (T-4) and the axially vacant trigonal bipyramid (vTBPY-4).

coordination polyhedra show a high dispersion in a shape map (Figure 16), indicative of deviations from the ideal octahedron.

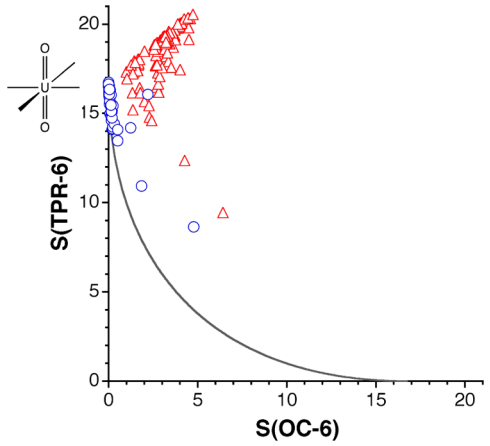

Figure 16. Shape measures of the experimental (triangles) and normalized (circles) coordination polyhedra of six-coordinate $[UO_2L_4]$ complexes with monodentate ligands, relative to the trigonal prism (TPR-6) and the octahedron (OC-6).

In contrast, the vast majority of the corresponding normalized polyhedra are grouped around the octahedron, with some of them presenting a slight degree of Bailar twist. The two outliers that occupy the lowest positions in the shape map shown are in fact complexes[50] in which the uranium atom is practically seven- rather than six-coordinated, with a pentagonal bipyramidal coordination geometry. The normalized polyhedra of related compounds of other actinides (not shown in Figure 16), much less abundant, appear all as practically perfect octahedra.

The heptacoordinate complexes of type $[UO_2L_5]$ with monodentate ligands appear mostly as pentagonal bipyramids, as clearly seen in a shape map of their normalized coordination polyhedra (Figure 17, left). However, a varying degree of distortion toward the capped trigonal prism can be appreciated, associated with the loss of coplanarity of the five nonoxo ligands, as seen by the nice correlation between the pentagonal shape measure of the L_5 group and the pentagonal bipyramidal shape measure of the whole coordination sphere. An outlier[51] deviates strongly from the pentagonal bipyramid and is practically midway along the path to the capped trigonal prism (lowest point in Figure 17). Probably the reason for such a unique stereochemistry is a weak coordination of a nitrogen atom that drives the coordination sphere toward an eight-vertex bicapped trigonal prism. It must be noticed that such an important stereochemical change requires only a moderate bending of the O═U═O bond angle, from 180° to 172°. The target capped trigonal prism seems to be one in which the two oxo groups occupy opposing vertices of a square face of the prism and one donor atom from a pentadentate ligand occupies the capping position, as schematically shown in Chart 4.

Chart 4

Analogous heptacoordinate complexes of other actinides (Pu and Np) with monodentate ligands present essentially the same stereochemical behavior as the uranium ones (Figure 17, right).

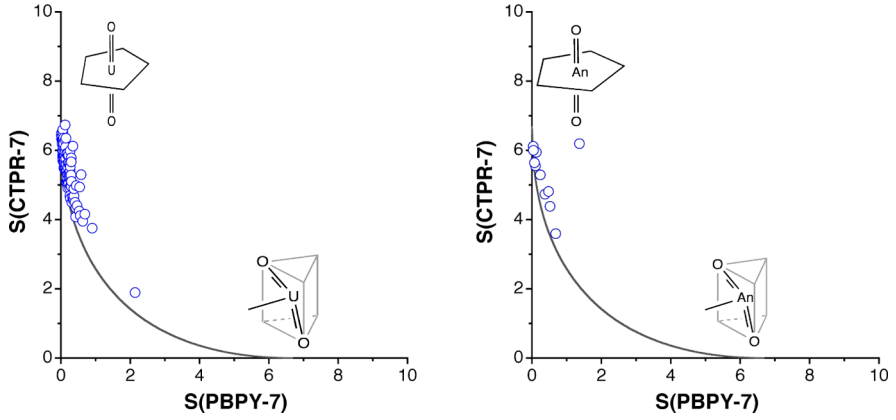

Figure 17. Left: Shape measures of the normalized coordination polyhedra of seven-coordinate $[UO_2L_5]$ complexes with monodentate ligands, relative to the capped trigonal prism (CTPR-7) and the pentagonal bipyramid (PBPY-7). Right: The corresponding shape map for complexes of Np and Pu.

dx.doi.org/10.1021/ic5021077 | *Inorg. Chem.* 2014, 53, 12151−12163

Compounds with bi- or multidentate ligands present a wider dispersion in their shape measures due to the geometrical constraints imposed by the chelate rings.

Shape measures of the normalized polyhedra of eight-coordinate $[UO_2L_6]$ complexes disclose a dominant hexagonal bipyramidal shape (Figure 18), with a number of complexes

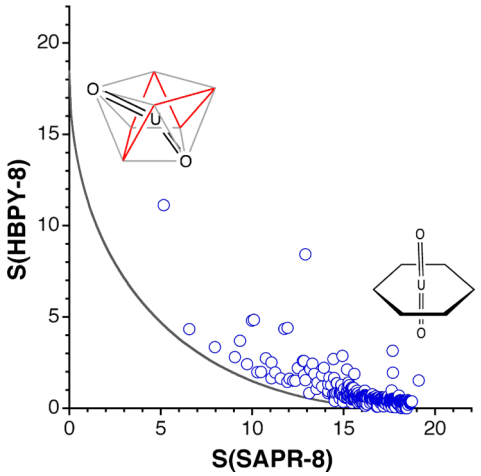

Figure 18. Shape measures of the normalized coordination polyhedra of eight-coordinate $[UO_2L_6]$ complexes relative to the square antiprism (SAPR-8) and the hexagonal bipyramid (HBPY-8).

aligned along the path for interconversion to the square antiprism. A similar behavior is found for the analogous complexes of other actinides (not shown).

J. Carbon Tetrahedricity in Haloalkanes. Although we have focused mainly on transition metal and actinide complexes, the continuous shape measures of normalized polyhedra can also be applied to organic stereochemical problems. As an example, we analyze here the degree of tetrahedricity of sp^3 carbon atoms in haloalkanes. Let us start by a single molecule, bromotricyanomethane,[52] whose central carbon atom has a high tetrahedral shape measure of 1.49. This value could in principle be taken as indicative of a significantly distorted tetrahedron. However, if we take into account that the C−Br bond distance is approximately 0.5 Å longer than the C−C distances, and we analyze the normalized coordination polyhedron, we find a shape measure of 0.08, indicative of nearly perfect tetrahedral bond angles. The two values taken together provide us with two clear stereochemical pieces of information: (i) the coordination polyhedron of that carbon atom is relatively far from being a regular tetrahedron, but (ii) that deviation comes from bond distance differences and not from an angular distortion.

If we extend this type of analysis to all sp^3 carbon atoms bonded to one Br and three C atoms, we find tetrahedral shape measures in the range 0.66−1.49 for the experimental, and 0.02−0.81 for the normalized coordination polyhedra. While it is clear that a large part of the deviation from the tetrahedron comes from bond distance differences, some compounds present non-tetrahedral structures even after removal of the bond distance distortions through normalization. We can therefore look at the angular distortions present in the normalized polyhedra by plotting them in a shape map (Figure 19, left), where we can appreciate that in most cases the deviation from the tetrahedral geometry can be reasonably attributed to a flattening distortion, given their closeness to the minimal distortion path to the square. The experimental structures appear much farther from that path because of the bond distance differences. We can thus see how the polyhedral normalization favors the stereochemical analysis of the family of XCR_3 compounds (X = halogen), informing us about the decrease of their path deviation upon normalization (Figure 19, right). As could be expected, the effect is most dramatic for the iodo derivatives and becomes almost negligible for the fluoro compounds (not shown in Figure 19 for clarity), since the difference between the C−X and C−C distances decreases as we move up in the halogen group, I > Br > Cl > F.

CONCLUSIONS

We have introduced the shape measures of normalized coordination polyhedra as a tool for the analysis of the stereochemistry around atoms having bonds of very different lengths due to, e.g., the presence of multiple bonds, substitution patterns with atoms of very different sizes, or the existence of secondary bonding. The joint analysis of the polyhedral shape measures of the experimental and normalized coordination polyhedra of an atom facilitates the task of telling the angular from the bond distance contributions to the distortion present in the experimental structure. A simple rule deduced here is that a decrease in the shape measure of a coordination

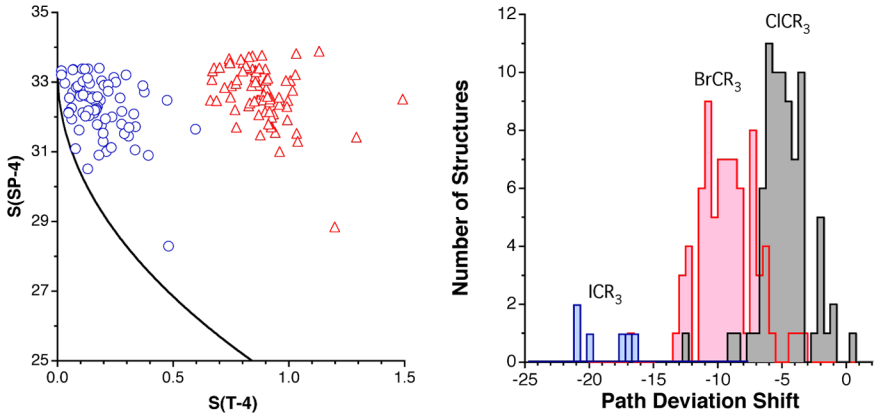

Figure 19. Left: Experimental (triangles) and normalized (circles) coordination polyhedra of carbon atoms in $BrCR_3$ groups plotted in a shape map relative to the tetrahedron and the square. Right: Changes in the deviation from the tetrahedral to square planar pathway upon normalization of the coordination polyhedra of sp^3 carbon atoms with an XC_3 environment (X = Cl, Br, I).

dx.doi.org/10.1021/ic5021077 | Inorg. Chem. 2014, 53, 12151−12163

polyhedron upon normalization is indicative of a bond shortening that preserves the bond angles of the ideal polyhedron, while an increase is diagnostic for an off-center shift of the central atom that introduces an angular distortion of the reference polyhedron.

In brief, these are the families of complexes that we have analyzed and the main conclusions regarding the shapes that best represent the stereochemistry of their normalized coordination polyhedra, which take into account only angular distortions:

(a) *cis*-$[MO_2L_4]$ complexes have shapes along the distortion path between the octahedron and the bicapped tetrahedron.

(b) $[X{\equiv}ML_5]$ complexes appear to be octahedral, distorted toward the pentagonal pyramid, probably associated to incipient coordination of a seventh ligand at the open side of the pyramid, favored by small bite bidentate ligands.

(c) $[O{=}ML_5]$ cores present distortions from the octahedron along the Bailar twist or toward a square pyramid with a weakly coordinated ligand, or combinations of these two distortions.

(d) $[X{\equiv}ML_4]$ complexes can be along the Berry pseudorotation pathway that connects the trigonal bipyramid and the square pyramid, or may present an umbrella distortion of a trigonal bipyramid that would extrapolate to a tetrahedral coordination sphere with an extra ligand capping a tetrahedral face at a long distance.

(e) $[MO_2L_3]$ complexes can be found along the Berry pathway or affected by an anti-Berry distortion of the trigonal bipyramid toward an edge-capped tetrahedron: those with a d^0 electron configuration (V^V, Mo^{VI}, W^{VI}, Re^{VII}, and Tc^{VII}) present anti-Berry structures, while those with d^2 configuration (Tc^V, Re^V, Ru^{VI}, Os^{VI}) exhibit Berry distortions. The complexes with coordinated alkyl groups are an exception to this rule, since they present agostic interactions that induce distortions that correspond to neither the Berry nor the anti-Berry pathways.

(f) In spite of the variety of five-coordinated Mo atoms found in oxido-reductases, regarding the number and arrangement of metal−ligand double bonds, their stereochemistries can be easily compared by means of their normalized coordination polyhedra. They are seen to be essentially square pyramidal, but deviations from that ideal geometry are common through non-Berry distortions associated with semicoordinating interactions or to a highly asymmetric angular distribution of the donor atoms, probably imposed by the protein backbone.

(g) $[X{\equiv}ML_3]$ complexes depart from the tetrahedral geometry, showing a variable degree of pyramidalization and spanning part of the pathway between the tetrahedron and the axially vacant trigonal bipyramid.

(h) $[UO_2L_4]$ uranyl complexes with monodentate ligands are nearly octahedral, and so are the similar complexes of Pu and Np.

(i) $[AnO_2L_5]$ actinyl complexes have nearly pentagonal bipyramidal geometries with varying degrees of distortion toward the capped trigonal prism.

(j) $[UO_2L_6]$ uranyl complexes have hexagonal bipyramidal shapes, distorted toward the square antiprism.

(k) The sp^3 carbon atom in haloalkanes, XCR_3, has a tetrahedral coordination with a slight degree of planarization distortion.

■ ASSOCIATED CONTENT

Supporting Information

Shape maps for the $MO_2L_2^{ax}$ group in *cis*-$[MO_2L_4]$, for pentacoordinate Mo and W $[O{=}M(dithiolene)_2]$ and $[S{=}M(dithiolene)_2]$ complexes, anti-Berry path for $[MoO_2(C_6F_5)_3]^-$ anion, and difference in path deviation functions relative to the octahedron−pentagonal pyramid and octahedron−trigonal prism paths for $[X{\equiv}ML_5]$ complexes. Computational Details. Inversion symmetry measures for compounds in Table 1, and atomic coordinates of optimized structures for $[RuO_2Ph_3]^-$, $[MoO_2Ph_3]^-$, $[RuO_2Cl_3]^-$, $[VO_2py_2F]$, $[VO_2py_2Cl]$, $[MoO_2Me_3]^-$, $[RuO_2Me_3]^-$, $[MoO_2H_3]^-$, and $[RuO_2H_3]^-$. This material is available free of charge via the Internet at http://pubs.acs.org.

■ AUTHOR INFORMATION

Corresponding Author

*E-mail santiago@qi.ub.es.

Notes

The authors declare no competing financial interest.

■ ACKNOWLEDGMENTS

This work was supported by the Spanish *Ministerio de Economía y Competitividad*, projects CTQ2011-23862-C02-01 and CTQ2011-23862-C02-02.

■ REFERENCES

(1) Alvarez, S.; Ruiz, E. In *Supramolecular Chemistry, From Molecules to Nanomaterials*; Steed, J. W., Gale, P. A., Eds.; John Wiley & Sons: Chichester, 2012; Vol. 5, pp 1993−2044;. Alvarez, S.; Alemany, P.; Casanova, D.; Cirera, J.; Llunell, M.; Avnir, D. *Coord. Chem. Rev.* **2005**, *249*, 1693.

(2) Alvarez, S.; Avnir, D.; Llunell, M.; Pinsky, M. *New J. Chem.* **2002**, *26*, 996.

(3) Neugebauer, D.; Fischer, E. O.; Dao, N. Q.; Schubert, U. *J. Organomet. Chem.* **1978**, *153*, C41.

(4) Arzoumanian, H.; Pierrot, M.; Ridouane, F.; Sanchez, J. *Transition Met. Chem.* **1991**, *16*, 422.

(5) Fenske, D.; Shihada, A.-F.; Schwab, H.; Dehnicke, K. *Z. Anorg. Allg. Chem.* **1980**, *471*, 1980.

(6) Esteruelas, M. A.; Modrego, F. J.; Oñate, E.; Royo, E. *J. Am. Chem. Soc.* **2003**, *125*, 13344.

(7) Werner, M.; Lis, T.; Bruhn, C.; Lindner, R.; Steinborn, D. *Organometallics* **2006**, *25*, 5946.

(8) Li, J.; Wang, G.; Shi, Z.; Yang, M.; Lluck, R. L. *Struct. Chem.* **2009**, *20*, 869.

(9) Herrmann, W. A.; Eder, S. J.; Scherer, W. *Chem. Ber.* **1993**, *126*, 39.

(10) Herrmann, W. A.; Roesky, P. W.; Kuhn, F. E.; Scherer, W.; Kleine, M. *Angew. Chem., Int. Ed.* **1993**, *32*, 1714.

(11) Bingham, A. L.; Drake, J. E.; Hursthouse, M. B.; Light, M. E.; Kumar, R.; Ratnani, R. *Polyhedron* **2006**, *25*, 3238.

(12) Bernhammer, J. C.; Huynh, H. V. *Organometallics* **2012**, *31*, 5121.

(13) Chamizo, J. A.; Morgado, J.; Castro, M.; Bernes, S. *Organometallics* **2002**, *21*, 5428.

(14) Douthwaite, R. E.; Green, M. L. H.; Silcock, P. J.; Gomes, P. T. *Organometallics* **2001**, *20*, 2611.

(15) Arnaiz, F. J.; Aguado, R.; Pedrosa, M. R.; De Cian, A. *Inorg. Chim. Acta* **2003**, *347*, 33.

(16) Ruiz-Martínez, A.; Casanova, D.; Alvarez, S. *Chem.—Eur. J.* **2010**, *16*, 6567.
(17) Allen, F. H. *Acta Crystallogr.* **2002**, *B58*, 380.
(18) Belsky, A.; Hellenbrandt, M.; Karen, V. L.; Luksch, P. *Acta Crystallogr.* **2002**, *B58*, 364.
(19) Lecomte, C.; Protas, J.; Richard, P.; Barbe, J. M.; Ruilard, R. *J. Chem. Soc., Dalton Trans.* **1982**, 247.
(20) Donahue, J. P.; Goldsmith, C. R.; Nadiminti, U.; Holm, R. *J. Am. Chem. Soc.* **1998**, *120*, 12869.
(21) Beck, J.; Strahle, J. *Z. Anorg. Allg. Chem.* **1987**, *554*, 50.
(22) García-Monforte, M. A.; Baya, M.; Falvello, L. R.; Martín, A.; Menjón, B. *Angew. Chem., Int. Ed.* **2012**, *51*, 8046.
(23) Edwards, A. J.; Steventon, B. R. *Chem. Commun.* **1967**, 462.
(24) Pinlac, R. A. F.; Stern, C. L.; Poeppelmeier, K. R. *Crystals* **2011**, *1*, 3.
(25) Taylor, J. C.; Waugh, A. B. *J. Chem. Soc., Dalton Trans.* **1980**, 2006. Taylor, J. C. *Z. Kristallogr.* **1987**, *181*, 151.
(26) Aldous, D. W.; Goff, R. J.; Attfield, J. P.; Lightfoot, P. *Inorg. Chem.* **2007**, *46*, 1277.
(27) Alvarez, S.; Llunell, M. *J. Chem. Soc., Dalton Trans.* **2000**, 3288.
(28) García-Monforte, M. A.; Baya, M.; Betoré, M. P.; Martín, A.; Menjón, B. *Dalton Trans.* **2014**, *43*, 7615.
(29) Casanova, D.; Cirera, J.; Llunell, M.; Alemany, P.; Avnir, D.; Alvarez, S. *J. Am. Chem. Soc.* **2004**, *126*, 1755.
(30) Mohan, M.; Bond, M. R.; Otieno, T.; Carrano, C. J. *Inorg. Chem.* **1995**, *34*, 1233.
(31) Cai, S.; Hoffman, D. M.; Wierda, D. A. *J. Chem. Soc., Chem. Commun.* **1988**, 313.
(32) Tatsumi, K.; Hoffmann, R. *Inorg. Chem.* **1980**, *19*, 2656.
(33) Kirk, M.; Stein, B. In *Comprehensive Inorganic Chemistry II*; Reedijk, J., Poeppelmeier, K. R., Eds.; Elsevier: Amsterdam, 2013; Vol. 3, pp 264−293.
(34) Romão, M. J. *Dalton Trans.* **2009**, 4053.
(35) Coelho, C.; Mahro, M.; Trincao, J.; Carvalho, A. T. P.; Ramos, M. J.; Terao, M.; Garattini, E.; Leimkuhler, S.; Romao, M. J. *J. Biol. Chem.* **2012**, *287*, 40690.
(36) Zander, U.; Faust, A.; Klink, B. U.; De Sanctis, D.; Panjikar, S.; Quentmeler, A.; Bardischewsky, F.; Friedrich, C. G.; Scheidig, A. J. *J. Biol. Chem.* **2011**, *286*, 8349. Pauff, J. M.; Cao, H.; Hille, R. *J. Biol. Chem.* **2009**, *284*, 8760. Okamoto, K.; Eger, B. T.; Nishino, T.; Pai, E. F.; Nishino, T. *Nucleosides, Nucleotides Nucleic Acids* **2008**, *27*, 888. Bailey, S.; Rapson, T.; Johnson-Winters, K.; Astashkin, A. V.; Kappler, U. *J. Biol. Chem.* **2009**, *284*, 2053. Kappler, U.; Bailey, S.; Feng, C.; Honeychurch, M. J.; Hanson, G. R.; Bernhardt, P.; Tollin, G.; Enemark, J. *Biochemistry* **2006**, *45*, 9696. Kappler, U.; Bailey, S. *J. Biol. Chem.* **2005**, *280*, 24999. Unciuleac, M.; Warkentin, E.; Page, C. C.; Boll, M.; Ermler, U. *Structure* **2004**, *12*, 2249. Hanzelmann, P.; Dobbek, H.; Gremer, L.; Huber, R.; Meyer, O. *J. Mol. Biol.* **2000**, *301*, 1221. Fukunari, A.; Okamoto, K.; Nishino, T.; Eger, B. T.; Pai, E. F.; Kamezawa, M.; Yamada, I.; Kato, N. *J. Pharmacol. Exp. Theor.* **2004**, *311*, 519. Okamoto, K.; Matsumoto, K.; Hille, R.; Eger, B. T.; Pai, E. F.; Nishino, T. *Proc. Natl. Acad. Sci. U.S.A.* **2004**, *101*, 7931. Matsumoto, K.; Okamoto, K.; Ashizawa, N.; Nishino, T. *J. Pharmacol. Exp. Theor.* **2011**, *336*, 95. Okamoto, K.; Kawaguchi, Y.; Eger, B. T.; Pai, E. F.; Nishino, T. *J. Am. Chem. Soc.* **2010**, *132*, 17080. Pauff, J. M.; Zhang, J.; Bell, C. E.; Hille, R. *J. Biol. Chem.* **2008**, *283*, 4818. Cao, H.; Pauff, J. M.; Hille, R. *J. Biol. Chem.* **2010**, *285*, 28044. Cao, H.; Hall, J.; Hille, R. *Biochemistry* **2014**, *53*, 533. Cao, H.; Pauff, J. M.; Hille, R. *J. Nat. Prod.* **2014**, *77*, 1693. Ishikita, H.; Eger, B. T.; Okamoto, K.; Nishino, T.; Pai, E. F. *J. Am. Chem. Soc.* **2012**, *134*, 999.
(37) Dietzel, U.; Kuper, J.; Doebbler, J. A.; Schulte, A.; Truglio, J. J.; Leimkuhler, S.; Kisker, C. *J. Biol. Chem.* **2009**, *284*, 8768.
(38) Cao, H.; Hall, J.; Hille, R. *J. Am. Chem. Soc.* **2011**, *133*, 12414.
(39) Enroth, C.; Eger, B. T.; Okamoto, K.; Nishino, T.; Nishino, T.; Pai, E. F. *Proc. Natl. Acad. Sci. U.S.A.* **2000**, *97*, 10723.
(40) Truglio, J. J.; Theis, K.; Leimkuhler, S.; Rappa, R.; Rajagopalan, K. V.; Kisker, C. *Structure* **2002**, *10*, 115.
(41) Santos-Silva, T.; Ferroni, F.; Thapper, A.; Marangon, J.; Gonzalez, P. J.; Rizzi, A. C.; Moura, I.; Moura, J. J.; Romao, M. J.; Brondino, C. D. *J. Am. Chem. Soc.* **2009**, *131*, 7990.
(42) Rebelo, J.; Macieira, S.; Dias, J. M.; Huber, R.; Ascenso, C. S.; Rusnak, F.; Moura, J. J.; Moura, I.; Romao, M. J. *J. Mol. Biol.* **2000**, *297*, 135. Schneider, F.; Lowe, J.; Huber, R.; Schindelin, H.; Kisker, C.; Knablein, J. *J. Mol. Biol.* **1996**, *263*, 53. Yamaguchi, Y.; Matsumura, T.; Ichida, K.; Okamoto, K.; Nishino, T. *J. Biochem. (Tokyo)* **2007**, *141*, 513. Schrader, N.; Fischer, K.; Theis, K.; Mendel, R. R.; Schwarz, G.; Kisker, C. *Structure* **2003**, *11*, 1251. Boer, D. R.; Thapper, A.; Brondino, C. D.; Romão, M. J.; Moura, J. J. *J. Am. Chem. Soc.* **2004**, *126*, 8614. Rebelo, J.; Dias, J. M.; Huber, R.; Moura, J. J.; Romão, M. J. *J. Biol. Inorg. Chem.* **2001**, *6*, 791. Wagener, N.; Pierik, A. J.; Ibdah, A.; Hille, R.; Dobbek, H. *Proc. Natl. Acad. Sci. U.S.A.* **2009**, *106*, 11055.
(43) Qiu, J. A.; Wilson, H. L.; Pushie, M. J.; Kisker, C.; George, G. N.; Rajagopalan, K. V. *Biochemistry* **2010**, *49*, 3989.
(44) Okamoto, K.; Eger, B. T.; Nishino, T.; Kondo, S.; Pai, E. F.; Nishino, T. *J. Biol. Chem.* **2003**, *278*, 1848.
(45) Bray, R. C.; Adams, B.; Smith, A. T.; Richards, R. L.; Lowe, J.; Bailey, S. *Biochemistry* **2001**, *40*, 9810.
(46) Bertero, M. G.; Rothery, R. A.; Boroumand, N.; Palak, M.; Ginet, N.; Weiner, J. H.; Strynadka, N. C. J. *J. Biol. Chem.* **2005**, *280*, 14836.
(47) Herrmann, W. A.; Baratta, W.; Herdtweck, E. *Angew. Chem., Int. Ed.* **1996**, *35*, 1951.
(48) Krivovichev, S. V. In *Comprehensive Inorganic Chemistry II*; Reedijk, J., Poeppelmeier, K. R., Eds.; Elsevier: Amsterdam, 2013; Vol. 2, pp 611−640.
(49) Alvarez, S.; Menjón, B. *Angew. Chem., Int. Ed.* **2014**, *53*, 2810.
(50) Navaza, A.; De Rango, C.; Charpin, P. *Acta Crystallogr., Sect. C: Cryst. Struct. Commun.* **1983**, *39*, 1625. Ok, K. M.; O'Hare, D. *J. Solid State Chem.* **2007**, *180*, 446.
(51) Steinhauser, G.; Giester, G.; Wagner, C.; Weinberger, P.; Zachhuber, B.; Ramer, G.; Villa, M.; Lendl, B. *Inorg. Chem.* **2012**, *51*, 6739.
(52) Witt, J. R.; Britton, D.; Mahon, C. *Acta Crystallogr., Sect. B: Struct. Crystallogr. Cryst. Chem.* **1972**, *28*, 950.